Materials Research. 2022; 25(suppl. 2): e20220143
DOI: https://doi.org/10.1590/1980-5373-MR-2022-0143

Bio-based Carbon Electrochemically Decorated with Cu Nanoparticles: Green Synthesis and Electrochemical Performance

Beatriz Carvalho da Silva Fonseca[a]*, *Luana Santos Araújo*[b], *Bárbara da Silva Pinheiro*[a], *Alan Silva dos Santos*[c], *Gisele Amaral-Labat*[a], *Jorge Tadao Matsushima*[d], *Maurício Ribeiro Baldan*[a]

[a]*Instituto Nacional de Pesquisas Espaciais, Coordenação de Pesquisas e Desenvolvimento Tecnológico (COPDT), São José dos Campos, SP, Brasil.*
[b]*Universidade Federal de Minas Gerais, Departamento de Física, Instituto de Ciências Exatas (ICEx), Belo Horizonte, MG, Brasil.*
[c]*Instituto Tecnológico de Aeronáutica, Departamento de Química, São José dos Campos, SP, Brasil.*
[d]*Faculdade de Tecnologia Prof. Jessen Vidal, São José dos Campos, SP, Brasil.*

Received: March 19, 2022; Revised: July 9, 2022; Accepted: August 01, 2022

This study aimed to synthesize a composite material composed of bio-based, porous carbon matrix and Cu nanoparticles through a simple, low-cost, and environmentally friendly method. Concentrated Kraft black liquor was used as a carbon precursor, and Cu nanoparticles were homogeneously deposited on the carbon matrix using electrochemical deposition. The textural properties determined using N_2 isotherms indicated increased surface area of a carbon matrix with a micro-mesoporous structure. Voltammetric tests demonstrated that the composite exhibited catalytic properties for electrochemical CO_2 reduction. Compared to the bio-based, porous carbon sample (C matrix), the bio-based carbon electrode electrochemically decorated with Cu nanoparticles (C–Cu composite) exhibited increased current values of approximately 2.4 times, a potential shift of approximately 90 mV, and an onset potential of −1.02 V, under CO_2 saturation.

Keywords: *Carbon material, black liquor, copper nanoparticles, CO_2 reduction, electrochemical deposition.*

1. Introduction

Black liquor is a toxic, dark-colored byproduct of paper and pulp production, which can adversely affect water resources[1]. This alkaline effluent is primarily composed of dissolved lignin, minerals[2], cellulose, hemicellulose, sodium salts, sulfur compounds, and other components[3]. Black liquor is abundantly produced during the Kraft pulping process, wherein the production of 1 ton of pulp generates approximately the same amount of black liquor[3]. The considerable production of black liquor warrants research into economically viable and environmentally friendly methods of disposal[1], which otherwise would undergoes incineration in industrial boilers for energy generation[4]. The lignin, cellulose, and hemicellulose from black liquor may react with formaldehyde during polymerization reactions under alkaline conditions at room temperature[3]. An alternative approach to augment and regulate the environmental impact of black liquor is its use for the production of new porous carbonaceous materials[1], as lignin is composed of phenylpropane units, which are highly reactive[5] and have a high carbon yield[6].

New carbon-based materials, such as graphene derivatives, have extensive applications, for example, as electrodes in supercapacitor[7,8] and materials for microwave electromagnetic interference[9], energy conversion and storage[10,11], and gas sensors[12]. However, these materials are generally produced from non-renewable resources through multiple steps, thereby increasing their final cost. Therefore, cost-effective carbonaceous materials derived from black liquor have been used for electromagnetic wave absorption[13,14], as an electrocatalyst support for fuel cells[3], for adsorption of heavy metals[15-17] and antibiotics[15], in electrical systems[18], and for energy storage[19].

Simultaneously, Cu-based electrocatalysts can be obtained using a simple, fast, and low-cost electrochemical deposition process, while producing non-toxic products in an aqueous medium at room temperature and minimizing environmental impact. This procedure is cost-effective compared to other processes, such as evaporation deposition, chemical reduction, and mechano-chemical synthesis[20]. In this technique, lower potential facilitates electrodissolution of Cu into Cu^{2+} ions in the presence of ascorbic acid, which acts as the reducing agent[20]. Briefly, a potential is applied that induces the oxidation of the Cu plate to Cu^{2+} species, and the reducing agent promotes the reduction of Cu^{2+} to Cu^0, leading to the nucleation step, followed by the growth phase, to generate Cu particles[20].

Electrochemical CO_2 reduction has been extensively studied to convert CO_2 into chemicals and fuels[21-27]. This process

*e-mail: beatriz.csilvafonseca@gmail.com

includes a simple experimental setup, with great potential for a large-scale applications[21], besides the possibility to use renewable energy to support the system[22,28-32]. However, to ensure commercial viability, it is essential to identify ways to overcome high thermodynamic stability of the CO_2 molecule[21,33,34] and direct it towards the formation of a particular product[21], such as CO, formic acid or formate, CH_4, C_2H_4, ethanol, and acetate[21]. Another issue with this process is the H_2 evolution reaction, which exhibits rapid kinetics and competes with CO_2 reduction[21,26,34], generating more stable intermediates than those obtained from CO_2 reduction, such as CO or *COOH[26]. The development of active, selective, and durable electrocatalysts[21] can help overcome these obstacles and increase the efficiency of the CO_2 reduction process.

Cu-based electrocatalysts have reduced cost, high stability, high efficiency for CO_2 electroreduction[35], and effectively convert CO_2 into hydrocarbons[22,36,37]. Furthermore, Cu presents a moderate *CO-intermediate binding energy and can catalyze the conversion of CO_2 to CO, HCOOH, alcohols, and hydrocarbons[35], whereas other metals exclusively produce CO and $HCOO^-$[37]. Thus, Cu is able to convert CO_2 into C_2–C_3 hydrocarbons, whereas other metals are only capable of converting CO_2 into C_1 products[23]. Moreover, the addition of a porous matrix facilitates the diffusion process of reactive species and alter their selectivity[22]. Therefore, carbon-based materials can be used to anchor metallic Cu, thereby preventing particle aggregation and favoring catalytic activity[35]. Although few carbonaceous supports, such as carbon aerogel[22,34], graphene[31,38], and carbon nanotubes[39], have been used previously, their syntheses require multiple steps and is often expensive. Therefore, new carbonaceous supports derived from biomass are being explored[40,41]. In this regard, the findings of this study will contribute to the production of a carbon structure derived from industrial waste (black liquor) using a sustainable method.

Strategies to lower greenhouse gas emissions to reduce global warming were one of the important themes discussed at COP26 UN Climate Change Conference. This study can help address this issue in the following ways: (i) the employment of a byproduct to produce sustainable raw material for CO_2 reduction, thereby stimulating circular economy and increasing green jobs; (ii) the production of metal-based electrocatalyst using green synthesis; (iii) development of a sustainable strategy for CO_2 sequestration; and (iv) the conversion of CO_2 into value-added products.

This study describes the production of a Cu-based electrocatalyst supported on a bio-based carbon matrix using a simple, sustainable, and low-cost method. The bio-based carbon matrix was first synthesized from raw Kraft black liquor, and then Cu nanoparticles were electrochemically deposited on the carbon matrix without using toxic reagents. Thereafter, the physico-chemical, morphological, textural, and electrochemical properties of the renewable Cu-supported bio-based carbon matrix were determined.

To the best of our knowledge, this is the first study on the use of a porous carbon material, derived from black liquor, as an electrocatalyst support for electrochemical CO_2 reduction, the incorporation of Cu nanoparticles from Cu plates on porous carbon matrix using an environmentally friendly electrodeposition method, and the concentration of black liquor to obtain large surface area. Furthermore, as the spontaneous evaporation of black liquor is a simple method that does not involve activation agents and heating processes.

2. Experimental

2.1. Synthesis of bio-based carbon matrix (C matrix)

Raw Kraft black liquor was obtained from Suzano Papel & Cellulose (Mogi das Cruzes/SP, Brazil) and dried at room temperature for 10 d, which increased the solid content from 16% (w/w) to 25% (w/w). Next, solid content was estimated using gravimetric tests that encompassed weighing the sample before and after drying at 105 °C for 24 h (n = 3)[3]. Gravimetric tests were also performed for the received liquor sample for comparison.

Sustainable, bio-based, porous carbon was produced from 25.00 g of concentrated black liquor (25% solid content), which was mixed with 3.35 g of resorcinol using a magnetic stirrer at room temperature and pressure (25 °C, 1 atm) until resorcinol was dissolved completely. Then, 11.25 g of polymethylmethacrylate (PMMA) and 11.00 g of 37% aqueous solution of formaldehyde were added to the reaction medium and agitated until a solid gel was obtained. The solid gel was cured and dried under room conditions for 5 d. Thereafter, carbonization of this material was performed in a horizontal furnace at a heating rate of 5 °C min^{-1} until 900 °C for 2 h, under inert (N_2) atmospheric conditions. Finally, the bio-based, porous carbon material was washed with deionized water until a neutral pH was achieved, and a fine powder (C matrix) with a particle size of <38 μm was obtained. For comparison, a sample (CBL16) was prepared through the same procedure, but using raw black liquor with 16% solid content.

2.2. Synthesis of bio-based, porous carbon matrix decorated with Cu nanoparticles (C–Cu)

The process of Cu deposition on C matrix was performed at room temperature and pressure. A potential of 30 V was applied using a DC Power Supply (FA-1030 Instrutherm). Electrolytic medium was prepared by mixing 0.55 g of C matrix, 0.20 g of the reducing agent, i.e., vitamin C (ascorbic acid), and 60 mL of deionized water. A magnetic stirrer was used throughout the process. Two Cu plates were immersed in the dark-colored aqueous medium, and Cu deposition occurred on the C matrix within 20 min with N_2 bubbling. At the end of the process, the brownish aqueous medium was oven-dried at 110 °C, and the resulting composite was labeled as C–Cu. Figure 1 presents a schematic illustration of the synthesis of the C matrix and the C–Cu composite.

2.3. Characterization of the C matrix and the C–Cu composite

The morphology of the samples was evaluated using scanning electron microscope fitted with a field emission gun (FEG-SEM; TESCAN MIRA3N), in the SE mode at a voltage of 5 kV. The primary elements in the composite were quantified using a detector (Oxford X-MAX 50 EDS).

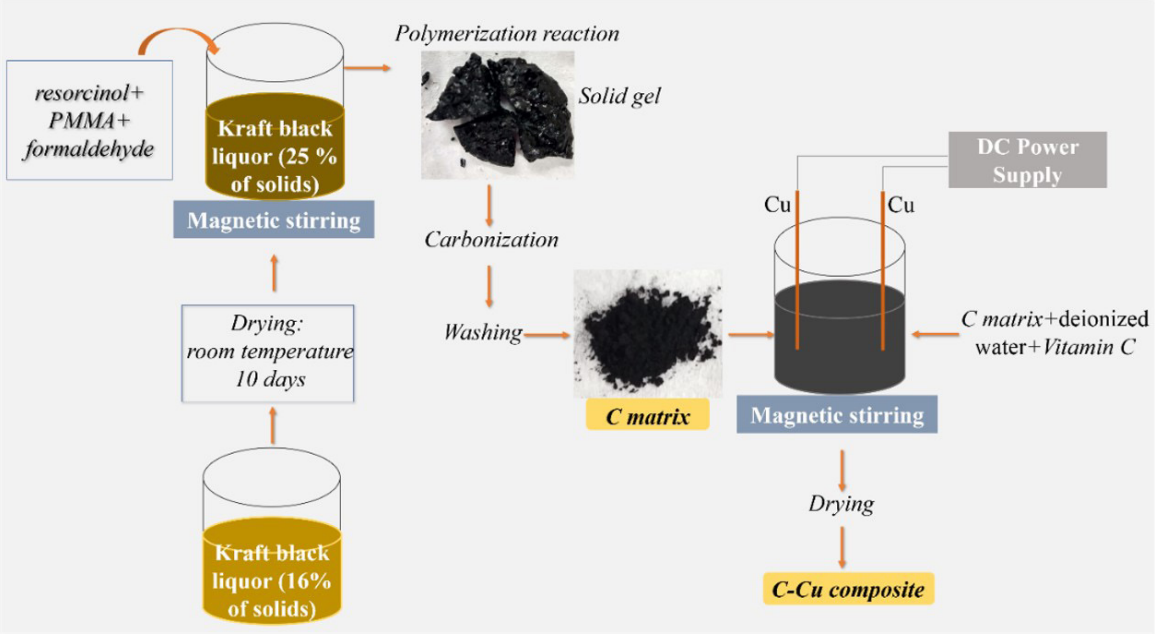

Figure 1. Schematic illustration of the synthesis of C matrix and C–Cu composite.

The porosity, surface area, and pore volume of the samples were determined through N_2 adsorption/desorption isotherm measurements at 77 K using the Micromeritics ASAP 2020 Plus equipment. First, the samples were subjected to a 24-h degassing process at 200 °C. Then, Brunauer–Emmet–Teller (BET) method was used to calculate the specific surface area (S_{BET})[42], whereas micropore volume (V_{DR}) was evaluated using the Dubinin–Radushkevic method[43]. The mesopore volume was estimated as $V_{0,97-}V_{DR}$, and pore-size distribution was calculated using the density functional theory (DFT)[44].

The crystalline structure and phase composition of the samples were analyzed by X-ray diffraction (XRD) using a diffractometer (PANalytical series X'PertPRO), with CuK-α radiation (α = 0.154056 nm) from 10º to 100º in 2-theta at a voltage of 40 kV, current of 30 mA, step size of 0.02º, and a counting time of 15 s per step.

2.4. Catalytic activity

The catalytic activity of the samples for electrochemical CO_2 reduction was evaluated by linear sweep voltammetry (LSV) measurements conducted using a potentiostat (Solartron analytical 1470E) with three-electrode cell configuration. A rectangular Pt electrode was used as the counter electrode, and Ag/AgCl system was used as the reference electrode. The working electrodes (C matrix and C–Cu composite) were deposited on a graphite plate, after blending 15 mg of sample, 100 µL of ethanol, 100 µL of 5% Nafion®, and 400 µL of deionized water. This suspension was prepared by ultrasonic agitation and dried at 100 °C after deposition. Subsequently, electrochemical measurements were performed using 30 mL of aqueous electrolyte $KHCO_3$ (1 mol L^{-1}) in a cell previously purged with N_2, and then CO_2 was added to the medium (45 mL min^{-1}).

3. Results and Discussion

3.1. Morphology, composition, and structural properties

FEG-SEM was employed to evaluate the morphology of the C matrix and the C–Cu composite. Figures 2a,b show the FEG-SEM images of the C matrix with uniformly distributed pores throughout its rough surface. Spherical Cu nanoparticles (red arrows) were homogenously dispersed on the sustainable carbon source, as shown in Figures 2c,d. Figure 3 presents a broad particle-size distribution of Cu particles on the C–Cu composite, with an average diameter of approximately 161 nm and a great amount of particle sizes <100 nm. The surface morphology of the C–Cu composite was also evaluated using EDS analysis and elemental mapping, as shown in Figures 4 and 5, respectively.

EDS spectrum not only indicated the presence of C and O in the C matrix, with Na and S as impurities from the delignification process[3], but also verified the presence of Cu (Figure 4). The weight percentage (wt.%) indicates elemental content (Figure 4). In addition, elemental mapping was performed using the EDS spectrum to evaluate the spatial distribution of C, Cu, and O on the C–Cu composite (Figure 5). As expected, C and O were present on the C matrix. Furthermore, the electrochemically decorated Cu nanoparticles were uniformly distributed on the surface of the bio-based, porous carbon material. Figure 6 shows XRD patterns for the C matrix and the C–Cu composite.

The spectrum of the C–Cu composite verified the formation of Cu^0 (00-002-1225/00-004-0836) in the carbonaceous material after deposition. The diffraction angles were identified at 43.25°, 50.35°, 74.04°, 89.87°, and 95.07°, corresponding to the planes (111), (200), (220), (311), and (222), respectively, as previously reported[22,31,34,45,46]. These results confirm that ascorbic acid reduced the oxide to its metallic form. The C

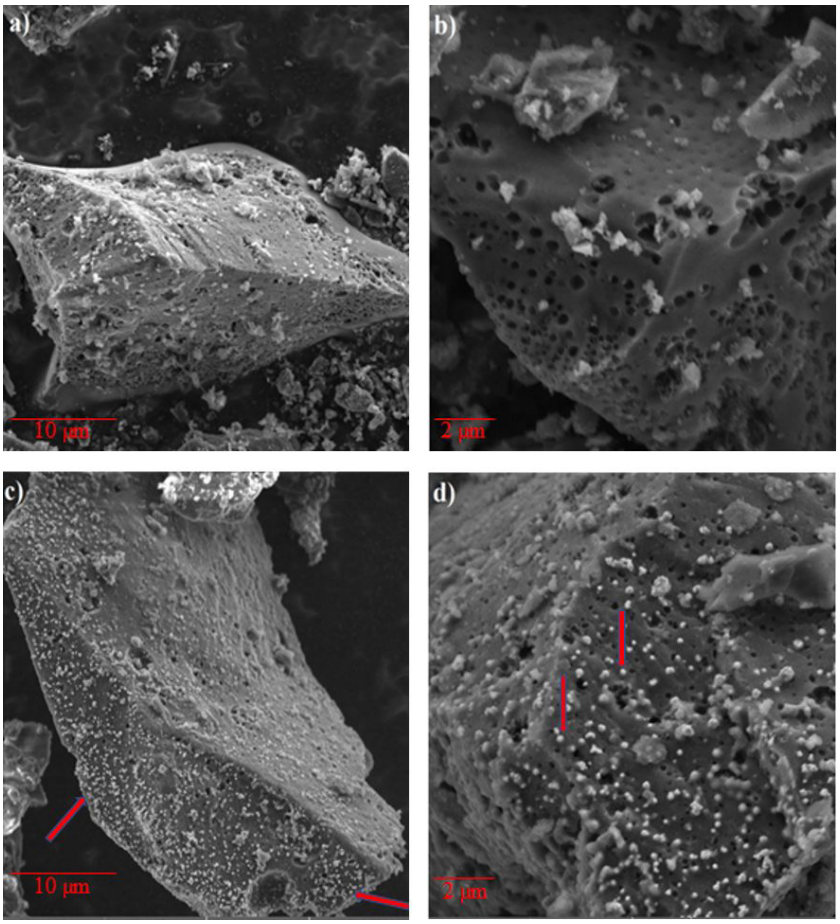

Figure 2. FEG-SEM images of the C matrix (a–b) and the C–Cu composite (c–d).

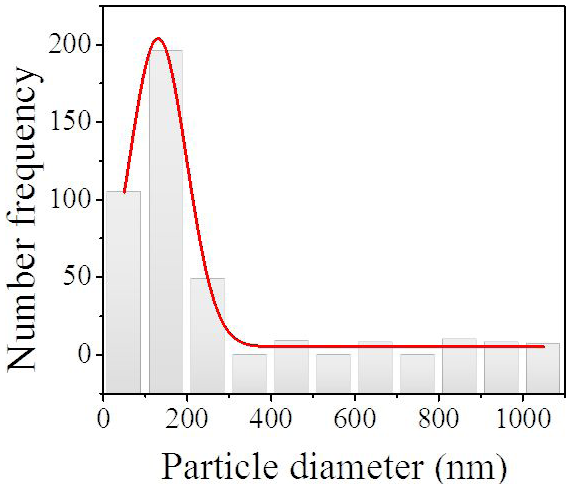

Figure 3. Particle-size distribution of Cu micro- and nanoparticles on the C–Cu composite.

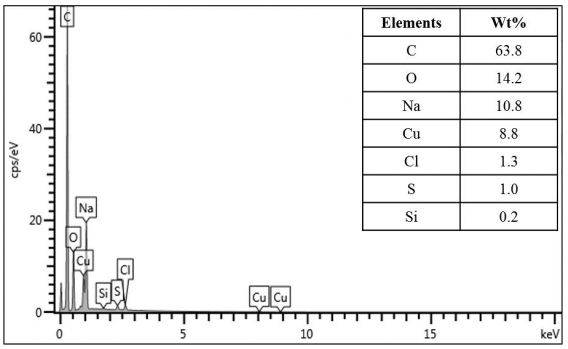

Elements	Wt%
C	63.8
O	14.2
Na	10.8
Cu	8.8
Cl	1.3
S	1.0
Si	0.2

Figure 4. EDS spectrum of the C–Cu composite.

matrix presents characteristic peaks of amorphous carbon structure around 25° and 44°, corresponding to (002) and (101)[13]. Additionally, most of the low intensity peaks in the diffractogram of the C matrix were probably related to inorganic matter from biomass ashes, such as chlorocalcite ($KCaCl_3$) (00-021-1170)[13], and the two remaining peaks can be associated with sulfur compounds (S 01-076-0183/ SCl_2 01-077-0296/ Na_2S_5 01-077-0294). These findings agree with those of the EDS spectrum.

3.2. Textural properties

Table 1 shows the textural properties of the C matrix and CBL16 samples and the C–Cu composite. Solid content increased from 16% to 25% by evaporation of the raw black liquor under room conditions, allowing a substantial increase

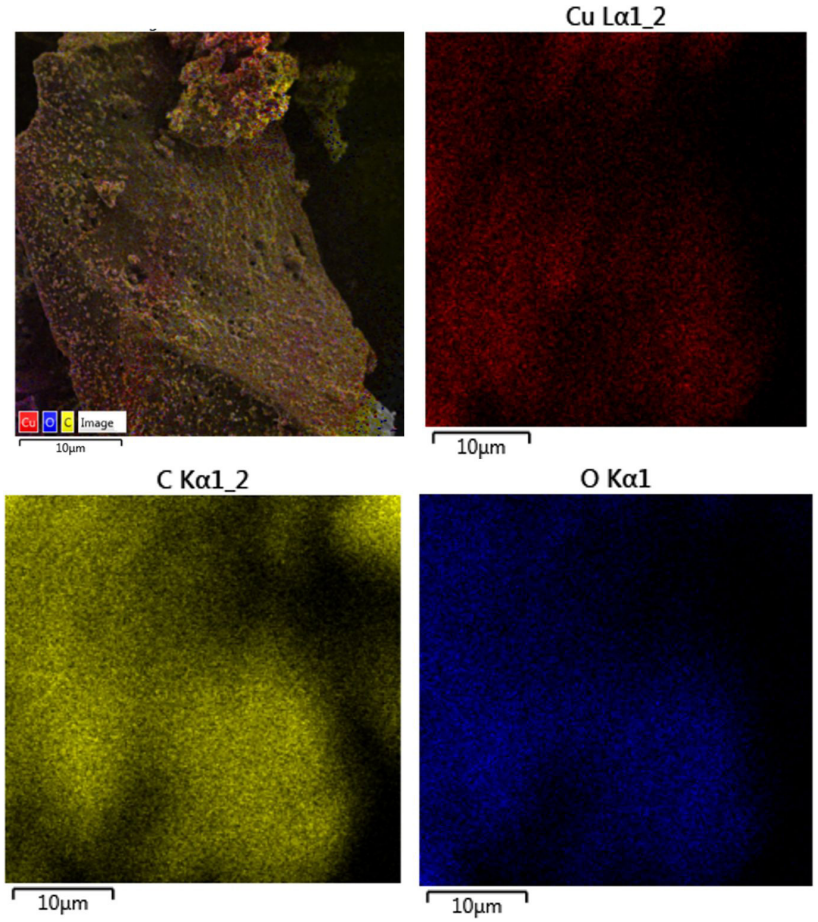

Figure 5. EDS analysis of the C–Cu composite.

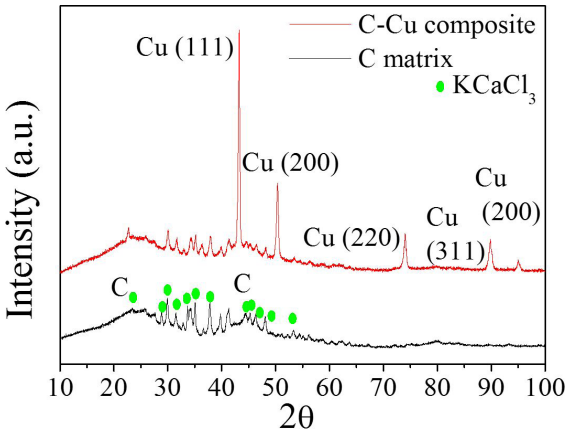

Figure 6. XRD spectra of C matrix and C-Cu composite.

in the surface area (121 $m^2 g^{-1}$). Total porosity constituted 58% of micropores and 42% of mesopores, exhibiting approximately equal proportions.

Previous studies report the use of black liquor as a precursor for different carbon materials, such as char, activated carbon, and porous carbon materials, which can be used for different purposes (Table 2). For increased porosity, these carbon materials undergo several preparatory steps, including hydrothermal processes, chemical reactions and carbonization under varying temperatures, and physical or chemical activation at various temperatures for different periods, which involve the use of gases (O_2), water vapor (H_2O), or chemicals (NaOH and KOH). Moreover, the latter requires several washing steps with HCl solutions and distilled water. The chemical activation process normally results in porous materials with large pore sizes compared to those obtained using physical activation process (Table 2), but multiple steps of preparation, such as the washing step, are always required. As a consequence, the final cost of the material increases.

Herein, the prepared non-activated porous carbon matrix exhibited an S_{BET} value 10 times higher than that of

Table 1. Surface area and pore volume of the CBL16, C matrix and the C–Cu composite.

Samples	S_{BET} (m^2g^{-1})	V_{TOTAL} (cm^3g^{-1})	V_{micro} (%)	V_{meso} (%)
CBL16	3	*	*	*
C matrix	121	0.08	58	42
C-Cu composite	7	0.01	*	*

*indeterminate

Table 2. Properties of porous carbon derived from black liquor.

Precursor	Product	Synthesis	Activation step	Activaction agent	S_{BET} (m^2g^{-1})	Reference
Evaporated Black Liquor	Activated Carbon	Carbonization/ Activation	Yes	Steam	310	[1]
Kraft Black Liquor and Tannin	Porous Carbon	Chemical and Hydrothermal Process	Yes	Oxygen	101	[47]
Evaporated Kraft Black Liquor	Porous Carbon	Carbonization/ Activation	Yes	KOH	1596	[15]
Kraft Black Liquor	Activated Carbon	Carbonization/ Activation	Yes	NaOH	2104	[19]
Evaporated Kraft Black Liquor	Char	Hydrothermal Process	No	-	12	[17]
Evaporated Kraft Black Liquor	Porous Carbon	Chemical/ Carbonization	No	-	121	This study

non-activated char prepared using hydrothermal synthesis. The surface area also exhibited the same order of magnitude compared to physically activated materials. Furthermore, the proposed sustainable material was prepared through a simple process, involving a chemical reaction under room conditions and few chemicals, followed by a standard carbonization process. The preparation did not employ high pressure or temperature and activating agents during the polymerization reaction, and thus reduced the final cost of the catalyst. In addition, the procedure required crude black liquor without lignin extraction or purification, contributing to the completeness of the original polymer network of the macromolecule. Black liquor was only subjected to an air-drying process to improve concentration, and thus increased porosity. The total porosity was further achieved using PMMA and with an increase in solid content in black liquor. Moreover, in this study, no purification process was used. After polymerization reaction, the formed gel was dried under ambient conditions (25 °C, 1 atm), again avoiding the use of high pressures and temperature. Therefore, this method is more viable as it did not involve the use of additional chemicals (CO_2, HCl, and H_2SO_4) and the washing step[3] for the production of bio-based carbon.

The sustainable C–Cu composite exhibited a surface area (7 $m^2 g^{-1}$) comparable to that of the carbon xerogel-supported Cu (4 m^2 g^{-1})[36]. However, the latter was prepared using synthetic products in a resorcinol–formaldehyde system and metal acetate, while distributing metallic Cu on the external surface of the sample. Despite the non-microporous structure, the synthetic xerogel exhibited electrocatalytic activity during the formation of hydrocarbons, primarily CH_4[36].

Metal loading onto a carbon support generally results in a decrease in the surface area and total pore volume of the matrix, suggesting a partial pore blockage by the metal particles[48]. However, the highest electrocatalytic CO_2 reduction efficiency might be achieved using a sample with the lowest surface area[48]. This behavior has been reported for nanostructured carbon nanotube that is used as an electrocatalyst support. Furthermore, increasing Cu content evidently decreased porosity, but the conversion of CO_2 into methanol was successful[49]. Therefore, the decreased surface area of the C–Cu composite suggests that Cu nanoparticles blocked the smallest pores on the carbon material, since the number of Cu particles <100 nm was high (Figure 3).

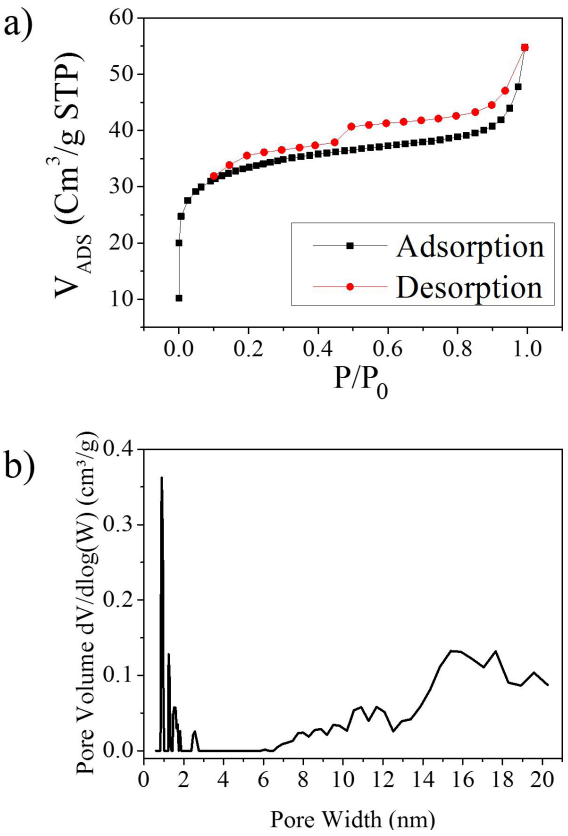

Figure 7. (a) N_2 adsorption–desorption isotherm of the C matrix, and (b) pore-size distribution estimated using the DFT method.

Figure 7a illustrates the N_2 isotherm of the precursor C matrix. According to the IUPAC report[50], the isotherm corresponds to a combination of types I and IV, suggesting the presence of micro- and mesopores, characteristic of carbonaceous materials derived from carbon-rich residues[3,51]. Furthermore, hysteresis-loop type H4 has been attributed to micro-mesoporous materials[50].

The pore-size distribution estimated using the DFT model (Figure 7b) revealed micropores centered at 0.9, 1.2, and 1.5 nm, while mesoporosity was identified in two distinct areas, the first being a peak centered at 2.5 nm and the second being a large distribution ranging from 7 nm to 20 nm, which

was in agreement with the isotherm. The average pore width, calculated as $4Vp/S_{BET}$[52], was 2.64 nm.

3.3. Catalytic activity for electrochemical CO_2 reduction

LSV measurements were performed to determine the electrocatalytic activity of the C matrix and the C–Cu composite for electrochemical CO_2 reduction. Figure 8a illustrates the LSV curves of the porous C matrix under N_2 bubbling and then under CO_2 saturation in an aqueous solution of 1.0 mol L^{-1} $KHCO_3$. LSV curves under N_2 bubbling are important to compare electrocatalytic activities with and without the presence of CO_2. Furthermore, N_2 bubbling eliminates O_2 in solution and prevents parallel competitive reactions of H_2 evolution, while CO_2 saturation establishes the equilibrium between CO_2 and HCO_3^- species. As shown in the LSV curves, the current values in the potential range of 0.2 V to −1.6 V at 5 mV s^{-1} established three regions of negative current labeled (I), (II), and (III). The region (I) corresponds to the typical current of double electric layer charging, whereas the region (III) is related to bulk H_2 evolution, indicating the same current values with a small difference corresponding to region (II). In this region, lower current values were observed for measurements under CO_2 saturation. This can be attributed to the alteration in the double electric layer arrangement owing to the presence of CO_2 or HCO_3^- species. These species are formed as a result of the equilibrium established during CO_2 saturation and implies a decrease in the formation of adsorbed H_2 from water reduction that occurs at more positive potentials.

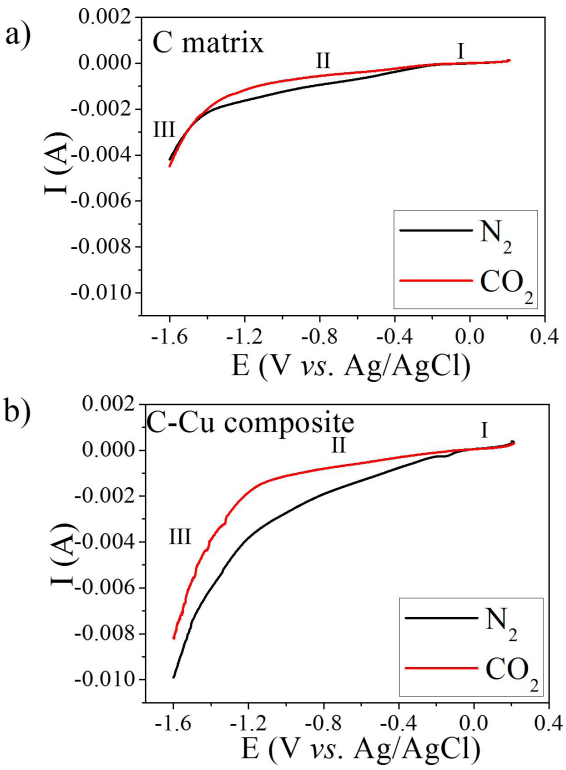

Figure 8. Linear sweep voltammetry curves of (a) the C matrix and (b) the C-Cu composite under N_2- and CO_2-saturated electrolytes.

A competitive reaction of H_2 evolution is expected in aqueous electrolytes during CO_2 conversion. Simultaneously, the existence of absorbed H_2 onto the catalyst surface is necessary for CO_2 activation[53]. Therefore, for an effective system, the amount of H_2 must be close to the stochiometric value for CO_2 hydrogenation to prevent parallel reactions[53]. Despite the formation of adsorbed H_2 under CO_2 saturation, indicated by the LSV curves (Figure 8a), CO_2 activation onto the porous C electrode was not verified, since CO_2 hydrogenation and, consequently, the suppression of H_2 evolution was not observed, as shown in region III.

The influence of the C–Cu composite was used to compare the current values resulting from the LSV curves illustrated in Figures 8a,b. An increase in current values to approximately 2.4 times was reported for the C–Cu composite, demonstrating increased effectiveness over H_2 evolution, as a well direct influence on CO_2 electroreduction. The effectiveness of Cu nanoparticles for CO_2 reduction is described by the combination of low-index crystal facets and coordination sites such as the corners, edges, and defects in Cu nanoparticles. Regarding CO_2 reduction, those parameters are crucial for the distribution of the gas phase of CO_2 and determines selectivity and sensitivity. Such crystallographic characteristics are expected to be dominant in C_2 products[54]. Tang et al.[55] suggested that the electrodeposited 50–110-nm Cu nanoparticles on a Cu electrode demonstrated higher selectivity toward C_2H_4 production upon CO_2 electrolysis in 0.1 mol L^{-1} $KClO_4$. According to Pérez-Cadenas et al.[36], Cu nanoparticles supported on carbon xerogels converted CO_2 into CH_4, C_2H_6, C_3H_4, C_3H_8, and C_3H_6 at −1.65 V using an Ag/AgCl system. Hence, a high quantity of products can be produced using Cu nanoparticles as the catalyst in CO_2-based electrochemical reactions.

As shown in Figure 8b, the C–Cu composite affected the processes occurring in regions II and III. Under CO_2 saturation, a decrease in the current values was associated with these regions. As indicated previously, this decrease might be associated with the presence of adsorbed H_2 that was completely consumed during CO_2 hydrogenation (region II). Consequently, CO_2 hydrogenation probably suppressed H_2 evolution, suggested by the decrease in current values of region III. Thus, LSV results confirm that there was a competition between H_2 evolution and CO_2 reduction for the electrolyte saturated with CO_2, indicating a decrease of H_2 evolution with CO_2 saturation. Similar results have been reported by Kaneco et al.[56] and Chang et al.[57], wherein Cu electrode exhibited a substantially lower current in CO_2-saturated electrolyte compared to N_2-saturated electrolyte. Moreover, the LSV results provide evidence for the sensitivity and selectivity of the C–Cu composite for CO_2 reduction.

Figure 9 shows the comparison in the activities of the C matrix and C–Cu composite samples under CO_2 saturation. For the C–Cu electrode, a shift in potential of approximately 90 mV was observed from the onset potential of approximately -1.02 V, in contrast to -1.11 V that was observed for the C matrix. This shift was correlated with electrocatalytic activity and suggested an improved CO_2 electroreduction performance. Xiao et al.[34] generated Cu nanoparticles dispersed on activated carbon aerogel, which exhibited remarkable CO Faradaic efficiency (75.6%) and the lowest

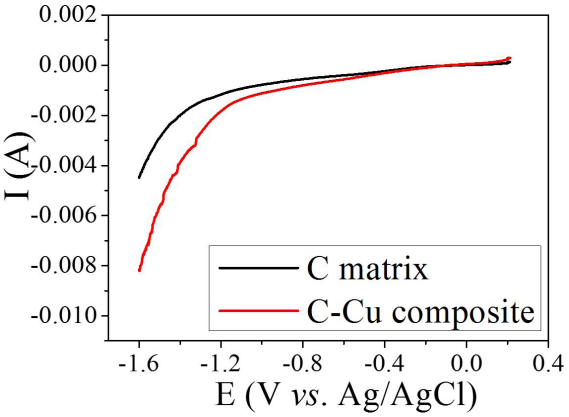

Figure 9. Linear sweep voltammetry curves of the C matrix and the C–Cu composite under CO_2 saturation.

onset potential during LSV analysis under CO_2 saturation. In another work, the onset potential of Cu nanoparticles decorated on pyridoxine modification graphene oxide sheets used for electrochemical CO_2 reduction to ethanol exhibited a significant positive shift. This catalyst showed superior catalytic ability for ethanol generation (FE ethanol = 56.3%) using CO_2-saturated 0.1 mol L^{-1} $KHCO_3$ aqueous solution[31]. In the previous studies, the Cu nanoparticles were generated by chemical deposition. Therefore, the active sites provided by Cu nanoparticles electrochemically decorated on C matrix assisted the high electrocatalytic ability of the C–Cu composite to catalyze CO_2, compared to the C matrix.

The mechanism underlying electrochemical CO_2 reduction is still debatable[37]; however, some pathways have been suggested. One of them considers CO_2 and HCO_3^- as reactants species and a separation between the formation of $HCOO^-$ (directly from CO_2 or HCO_3^-) and CO (directly from CO_2) to affect electrochemical CO_2 reduction. Furthermore, species, such as C_2H_4, C_2H_6, and CH_4, can also be obtained from CO intermediates[37]. Ma et al.[58] proposed a reaction pathway for the electrocatalytic activity of CO_2 supported on Cu nanowire arrays for the formation of $HCOO^-$, C_2H_4, C_2H_6, CH_4, CO, and CH_3CH_2OH, with evidence from two routes; one with products derived from COH formation and the second with products derived from CO dimerization. It is reinforced that CO is a key intermediate for the formation of hydrocarbons, although the rate-determining step in the conversion of CO_2 to CO is the first electron transfer for the formation of the $CO_2^{\cdot-}$ intermediate[58]. All these products are reported for Cu-based electrodes with previously mentioned starting conditions, thus, the reactions performed using the C–Cu composite possibly follow similar mechanisms.

Therefore, the composite constituted by Cu, a non-noble and cheap electrocatalyst, is a promising material towards a sustainable future. Firstly, Cu foil is a competitively priced material compared to other metals used for CO_2 electroreduction, such as Au and Ag. As shown in Table 3, Cu costs 1.2 times lesser than Ag and 34 times lesser than Au, providing an excellent candidate for electrochemical applications, as the price of the electrocatalyst notably affects the final cost of the material. Secondly, the electrochemical deposition was performed on a bio-based, highly renewable C matrix.

Table 3. Comparison of the costs of 0.25-mm-thick Cu, Ag, and Au foils with an area of 25 cm^2 (Sigma Aldrich).

Foil	Code	Price ($)
Cu	349178-25 cm^2	68.10
Ag	326984-25 cm^2	82.90
Au	349240-12G	2,290.00

Therefore, Cu electrodeposition on a sustainable matrix using Cu foil is a green synthesis method based on a straightforward process that involves low-cost, non-toxic reagents.

4. Conclusions

In this study, a bio-based, porous carbon material was prepared from concentrated Kraft black liquor using a simple, low-cost, and sustainable method, where Cu nanoparticles were electrochemically deposited on the carbon surface using a low-cost environmentally friendly system. We verified that concentrated black liquor increased the surface area and pore volume of the matrix, thereby creating micro- and mesopores in approximately equal proportions. The electrodeposition method homogeneously distributed Cu nanoparticles on the surface of the C matrix. However, the nanoparticles probably obstructed the small pores (<100 nm), indicated by the reduced surface area after Cu deposition. The nanoparticles were mainly composed of metallic Cu, which probably created active sites on the material surface, and consequently, increased the cathodic current in the voltammetric tests. The results suggested an interaction of the C–Cu composite with CO_2 and/or products derived from CO_2 electroreduction, resulting from decreased H_2 evolution, which may have contributed to CO_2 activation. Therefore, the sustainable porous C–Cu composite is an attractive material for CO_2 electroreduction. Furthermore, the material was synthesized using green chemistry, by reusing an industrial waste (black liquor) to generate a new porous material using a simple method and, simultaneously, utilizing one of the most important greenhouse gas, CO_2, in agreement with the COP26 issues.

5. Acknowledgments

This study was supported by the following Brazilian research agencies: Coordenação de Aperfoiçoamento de Pessoal de Nível Superior – Brasil (CAPES) – Finance code 001 (grant n° 88882.444518/2019-01), CNPq, and FINEP.

6. References

1. Fu K, Yue Q, Gao B, Sun Y, Zhu L. Preparation, characterization and application of lignin-based activated carbon from black liquor lignin by steam activation. Chem Eng J. 2013;228:1074-82.
2. Boucard H, Weiss-Hortala E, Gueye F, Espitalier F, Barna R. Insights in mechanisms of carbonaceous microparticles formation from black liquor hydrothermal conversion. J Supercrit Fluids. 2020;161:104817.
3. Amaral-Labat G, da Silva EL, Cuña A, Malfatti CF, Marcuzzo JS, Baldan MR, et al. A sustainable carbon material from kraft black liquor as nickel-based electrocatalyst support for ethanol electro-oxidation. Waste Biomass Valoriz. 2021;12(5):2507-19.
4. Diehl BG, Brown NR, Frantz CW, Lumadue MR, Cannon F. Effects of pyrolysis temperature on the chemical composition

of refined softwood and hardwood lignins. Carbon N Y. 2013;60:531-7.
5. Seo J, Park H, Shin K, Baeck SH, Rhym Y, Shim SE. Lignin-derived macroporous carbon foams prepared by using poly(methyl methacrylate) particles as the template. Carbon N Y. 2014;76:357-67.
6. Zhu J, Yan C, Zhang X, Yang C, Jiang M, Zhang X. A sustainable platform of lignin: from bioresources to materials and their applications in rechargeable batteries and supercapacitors. Pror Energy Combust Sci. 2020;76:100788.
7. Kumar R, Sahoo S, Tan WK, Kawamura G, Matsuda A, Kar KK. Microwave-assisted thin reduced graphene oxide-cobalt oxide nanoparticles as hybrids for electrode materials in supercapacitor. J Energy Storage. 2021;40:102724.
8. Kumar R, Abdel-Galeil MM, Ya KZ, Fujita K, Tan WK, Matsuda A. Facile and fast microwave-assisted formation of reduced graphene oxide-wrapped manganese cobaltite ternary hybrids as improved supercapacitor electrode material. Appl Surf Sci. 2019;481:296-306.
9. Kumar R, Sahoo S, Joanni E, Singh RK, Tan WK, Kar KK, et al. Recent progress on carbon-based composite materials for microwave electromagnetic interference shielding. Carbon N Y. 2021;177:304-31.
10. Kumar R, Joanni E, Singh RK, Singh DP, Moshkalev SA. Recent advances in the synthesis and modification of carbon-based 2D materials for application in energy conversion and storage. Pror Energy Combust Sci. 2018;67:115-57.
11. Kumar R, Sahoo S, Joanni E, Singh RK, Maegawa K, Tan WK, et al. Heteroatom doped graphene engineering for energy storage and conversion. Mater Today. 2020;39:47-65.
12. Hashtroudi H, Kumar R, Savu R, Moshkalev S, Kawamura G, Matsuda A, et al. Hydrogen gas sensing properties of microwave-assisted 2D Hybrid Pd/rGO: effect of temperature, humidity and UV illumination. Int J Hydrogen Energy. 2021;46(10):7653-65.
13. Vergara DEF, Lopes BHK, Quirino SF, Silva GFBL, Boss AFN, Amaral-Labat GA, et al. Frequency selective surface properties of microwave new absorbing porous carbon materials embedded in epoxy resin. Mater Res. 2019;22(Suppl. 1):e20180834.
14. Bispo MC, Lopes BHK, Fonseca BCS, Portes RC, Matsushima JT, Yassuda MKH, et al. Electromagnetic properties of Carbon-Graphene Xerogel, Graphite and Ni-Zn Ferrite composites in polystyrene matrix in the X-Band (8.2 – 12.4 GHz). Materia. 2021;26(2):e12967.
15. Tian Y, Zhou H. A novel nitrogen-doped porous carbon derived from black liquor for efficient removal of Cr(VI) and tetracycline: comparison with lignin porous carbon. J Clean Prod. 2022;333:130106.
16. Gao Y, Yue Q, Gao B, Sun Y, Wang W, Li Q, et al. Preparation of high surface area-activated carbon from lignin of papermaking black liquor by KOH activation for Ni(II) adsorption. Chem Eng J. 2013;217:345-53.
17. Zhao Y, Tian Y, Zhou H, Tian Y. Hydrothermal conversion of black liquor to phenolics and hydrochar: characterization, application and comparison with lignin. Fuel. 2020;280:118651.
18. Foulet A, Birot M, Backov R, Sonnemann G, Deleuze H. Preparation of hierarchical porous carbonaceous foams from Kraft black liquor. Mater Today Commun. 2016;7:108-16.
19. Plavniece A, Volperts A, Dobele G, Zhurinsh A, Kaare K, Kruusenberg I, et al. Wood and black liquor-based N-doped activated carbon for energy application. Sustainability. 2021;13(16):9237.
20. Saini K, Shree Pandey R. Concentration-dependent electrochemical synthesis of quantum dot and nanoparticles of copper and shape-dependent degradation of methyl orange. Adv Mater Lett. 2017;8(11):1080-8.
21. Li L, Huang Y, Li Y. Carbonaceous materials for electrochemical CO_2 reduction. EnergyChem. 2020;2(1):100024.
22. Han X, Wang M, Le ML, Bedford NM, Woehl TJ, Thoi VS. Effects of substrate porosity in carbon aerogel supported copper for electrocatalytic carbon dioxide reduction. Electrochim Acta. 2019;297:545-52.
23. Wang Y, Niu C, Wang D. Metallic nanocatalysts for electrochemical CO2 reduction in aqueous solutions. J Colloid Interface Sci. 2018;527:95-106.
24. Sun Z, Ma T, Tao H, Fan Q, Han B. Fundamentals and challenges of electrochemical CO_2 reduction using two-dimensional. Mater Chem. 2017;3(4):560-87.
25. Fan Q, Zhang M, Jia M, Liu S, Qiu J, Sun Z. Electrochemical CO_2 reduction to C_{2+} species: heterogeneous electrocatalysts, reaction pathways, and optimization strategies. Mater Today Energy. 2018;10:280-301.
26. Ma T, Fan Q, Li X, Qiu J, Wu T, Sun Z. Graphene-based materials for electrochemical CO_2 reduction. J CO2 Util. 2019;30:168-82.
27. Yu J, Liu H, Song S, Wang Y, Tsiakaras P. Electrochemical reduction of carbon dioxide at nanostructured SnO_2/carbon aerogels: the effect of tin oxide content on the catalytic activity and formate selectivity. Appl Catal A Gen. 2017;545:159-66.
28. Li Q, Rao X, Sheng J, Xu J, Yi J, Liu Y, et al. Energy storage through CO_2 electroreduction: a brief review of advanced Sn-based electrocatalysts and electrodes. J CO2 Util. 2018;27:48-59.
29. Bashir S, Hossain SS, Rahman SU, Ahmed S, Al-Ahmed A, Hossain MM. Electrocatalytic reduction of carbon dioxide on SnO_2/MWCNT in aqueous electrolyte solution. J CO2 Util. 2016;16:346-53.
30. Wang S, Kou T, Baker SE, Duoss EB, Li Y. Recent progress in electrochemical reduction of CO2 by oxide-derived copper catalysts. Mater Today Nano. 2020;12:100096.
31. Yuan J, Yang MP, Zhi WY, Wang H, Wang H, Lu JX. Efficient electrochemical reduction of CO_2 to ethanol on Cu nanoparticles decorated on N-doped graphene oxide catalysts. J CO_2 Util. 2019;33:452-60.
32. Gang Y, Pan F, Fei Y, Du Z, Hu YH, Li Y. Highly efficient Nickel, Iron, and Nitrogen codoped carbon catalysts derived from industrial waste petroleum coke for electrochemical CO_2 reduction. ACS Sustain Chem& Eng. 2020;8(23):8840-7.
33. Lu Q, Jiao F. Electrochemical CO_2 reduction: electrocatalyst, reaction mechanism, and process engineering. Nano Energy. 2016;29:439-56.
34. Xiao X, Xu Y, Lv X, Xie J, Liu J, Yu C. Electrochemical CO_2 reduction on copper nanoparticles-dispersed carbon aerogels. J Colloid Interface Sci. 2019;545:1-7.
35. Yan Y, Ke L, Ding Y, Zhang Y, Rui K, Lin H, et al. Recent advances in Cu-based catalysts for electroreduction of carbon dioxide. Mater Chem Front. 2021;5(6):2668-83.
36. Pérez-Cadenas AF, Ros CH, Morales-Torres S, Pérez-Cadenas M, Kooyman PJ, Moreno-Castilla C, et al. Metal-doped carbon xerogels for the electro-catalytic conversion of CO_2 to hydrocarbons. Carbon N Y. 2013;56:324-31.
37. Lee S, Hong S, Lee J. Bulk pH contribution to CO/HCOO− production from CO_2 on oxygen-evacuated Cu_2O electrocatalyst. Catal Today. 2017;288:11-7.
38. Dongare S, Singh N, Bhunia H. Nitrogen-doped graphene supported copper nanoparticles for electrochemical reduction of CO_2. J CO2 Util. 2021;44:101382.
39. Irfan Malik M, Malaibari ZO, Atieh M, Abussaud B. Electrochemical reduction of CO_2 to methanol over MWCNTs impregnated with Cu_2O. Chem Eng Sci. 2016;152:468-77.
40. Gong S, Xiao X, Wang W, Sam DK, Lu R, Xu Y, et al. Silk fibroin-derived carbon aerogels embedded with copper nanoparticles for efficient electrocatalytic CO_2-to-CO conversion. J Colloid Interface Sci. 2021;600:412-20.
41. Costa RS, Aranha BSR, Ghosh A, Lobo AO, da Silva ETSG, Alves DCB, et al. Production of oxalic acid by electrochemical reduction of CO_2 using silver-carbon material from babassu coconut mesocarp. J Phys Chem Solids. 2020;147:109678.

42. Brunauer S, Emmett PH, Teller E. Adsorption of gases in multimolecular layers. J Am Chem Soc. 1938;60(2):309-19.
43. Dubinin MM. Fundamentals of the theory of adsorption in micropores of carbon adsorbents: characteristics of their adsorption properties and microporous structures. Carbon N Y. 1989;27(3):457-67.
44. Tarazona P. Solid-fluid transition and interfaces with density functional approaches. Surf Sci. 1995;331–333:989-94.
45. Cao Y, Moniri Javadhesari S, Mohammadnejad S, Khodadustan E, Raise A, Akbarpour MR. Microstructural characterization and antibacterial activity of carbon nanotube decorated with Cu nanoparticles synthesized by a novel solvothermal method. Ceram Int. 2021;47(18):25729-37.
46. Dong Y, Wang K, Tan Y, Wang Q, Li J, Mark H, et al. Synthesis and characterization of pure copper nanostructures using wood inherent architecture as a natural template. Nanoscale Res Lett. 2018;13(1):1-8.
47. Moreira WM, Viotti PV, Vieira MGA, Baptista CMSG, Scaliante MHNO, Gimenes ML. Hydrothermal synthesis of biobased carbonaceous composite from a blend of kraft black liquor and tannin and its application to aspirin and paracetamol removal. Colloids Surf A Physicochem Eng Asp. 2021;608:125597.
48. Lucas-Consuegra A, Serrano-Ruiz J, Gutiérrez-Guerra N, Valverde J. Low-temperature electrocatalytic conversion of CO_2 to liquid fuels: effect of the Cu particle size. Catalysts. 2018;8(8):340.
49. Safdar Hossain S, Rahman SU, Ahmed S. Electrochemical reduction of carbon dioxide over CNT-supported nanoscale copper electrocatalysts. J Nanomater. 2014;2014:1-10.
50. Thommes M, Kaneko K, Neimark AV, Olivier JP, Rodriguez-Reinoso F, Rouquerol J, et al. Physisorption of gases, with special reference to the evaluation of surface area and pore size distribution (IUPAC Technical Report). Pure Appl Chem. 2015;87(9-10):1051-69.
51. Amaral-Labat G, Munhoz MGC, Fonseca BCS, Boss AFN, de Almeida-Mattos P, Braghiroli FL, et al. Xerogel-like materials from sustainable sources: properties and electrochemical performances. Energies. 2021;14(23):7977.
52. Araújo TP, Quesada HB, Santos DF, Fonseca BCS, Barbieri JZ, Bergamasco R, et al. Acetaminophen removal by calcium alginate/activated hydrochar composite beads: batch and fixed-bed studies. Int J Biol Macromol. 2022;203:553-62.
53. Pérez-Rodríguez S, Sebastián D, Lázaro MJ, Pastor E. Stability and catalytic properties of nanostructured carbons in electrochemical environments. J Catal. 2017;355:156-66.
54. Baturina OA, Lu Q, Padilla MA, Xin L, Li W, Serov A, et al. CO_2 electroreduction to hydrocarbons on carbon-supported Cu nanoparticles. ACS Catal. 2014;4(10):3682-95.
55. Tang W, Peterson AA, Varela AS, Jovanov ZP, Bech L, Durand WJ, et al. The importance of surface morphology in controlling the selectivity of polycrystalline copper for CO_2 electroreduction. Phys Chem Chem Phys. 2012;14(1):76-81.
56. Kaneco S, Iiba K, Katsumata H, Suzuki T, Ohta K. Effect of sodium cation on the electrochemical reduction of CO_2 at a copper electrode in methanol. J Solid State Electrochem. 2007;11(4):490-5.
57. Chang TY, Liang RM, Wu PW, Chen JY, Hsieh YC. Electrochemical reduction of CO_2 by Cu_2O-catalyzed carbon clothes. Mater Lett. 2009;63(12):1001-3.
58. Ma M, Djanashvili K, Smith WA. Controllable hydrocarbon formation from the electrochemical reduction of CO_2 over Cu nanowire arrays. Angew Chem Int Ed. 2016;55(23):6680-4.